BJPS

Brazilian Journal of
Pharmaceutical Sciences

http://dx.doi.org/10.1590/s2175-97902022e20884

Determination of sunset yellow, allura red, and fast green using a novel magnetic nanoadsorbent modified with *Elaeagnus angustifolia* based on magnetic solid-phase extraction by HPLC

Tülay Oymak[1*], Emrah Dural[2]

[1]Department of Analytical Chemistry, Faculty of Pharmacy, Sivas Cumhuriyet University, Sivas, Turkey, [2]Department of Pharmaceutical Toxicology, Faculty of Pharmacy, Sivas Cumhuriyet University, Sivas, Turkey

Sunset yellow (SY), allura red (AR) and fast green (FG) are frequently used in commercial food products, although they are considered to be hazardous to public health due to their toxic efficacy and high exposure risk potency. In this study, a new, rapid, and reliable method based on a magnetic solid-phase extraction (MSPE) was developed for the simultaneous determination of SY, AR, and FG. Fe_3O_4 modified with *Elaeagnus angustifolia* was used for the first time as an adsorbent (Fe_3O_4-EA) in MSPE. It was characterized with scanning electron microscopy, Brunauer Emmet Teller surface area analysis and X-ray diffraction. MSPE parameters were optimized in terms of pH, adsorption, and elution time and elution volume. High-performance liquid chromatography was used for dye quantitation. Analytical separation was performed by applying ammonium acetate buffer, acetonitrile, and methanol as the mobile phase to a C_{18} reverse-phase analytical column. Intraday and inter-day repeatability of the method performed at the concentration of 0.2, 1.0 and 2.0 µg/mL exhibited <8.1% RSD (n=3). The limit of detection values was between 0.05-0.1 µg/mL. The adsorption data of SY, AR and FG on Fe_3O_4-EA were fitted with the Langmuir model with q_{max} values of 45.0, 70.4 and 73.0 mg/g, respectively.

Keywords: Food dyes. *Elaeagnus angustifolia*. Nanoparticles. Magnetic solid-phase extraction. HPLC-UV.

INTRODUCTION

Dyes are widely used as colorant agents in foodstuffs, and the pharmaceutical and cosmetics industries (Allam, Kumar, 2011; Tikhomirova, Ramazanova, Apyari, 2018; Vlase *et al*., 2014). Due to their low price, high effectivity and good stability, synthetic dyes are used more than natural dyes (He *et al.,* 2013; López-de-Alba, López-de-Martinez, De-León-Rodríguez, 2002; Mathiyalagan, Mandal, Ling, 2019). However, some synthetic dyes especially azo-dyes can be metabolized to harmful components in the human body. A number of studies have reported that many synthetic dyes have harmful effects on human health such as DNA damage (Amchova, Kotolova, Ruda-Kucerova, 2015; Sayed *et al*., 2012), genotoxic (Ali *et al*., 2020; Sayed *et al.,* 2012), carcinogenic (Amchova, Kotolova, Ruda-Kucerova, 2015), hyperactivity (Rovina *et al*., 2016), allergy (Amchova, Kotolova, Ruda-Kucerova, 2015; EFSA 2010), asthma (Yadav *et al*., 2012) reactions and behavioral hyperactivity in children (McCann *et al*., 2007). In order to ensure product safety, it is recommended that synthetic dyes in food and cosmetic products are monitored (De Andrade *et al*., 2014; Hu *et al*., 2017; Iammarino *et al*., 2019; Qin *et al*., 2019). However, it is challenging to determine the dyes simultaneously in various samples due to the complex matrix and the combination of a large number of dyes. Separation and pre-concentration are

---

***Correspondence:** T. Oymak. Department of Analytical Chemistry. Faculty of Pharmacy. Sivas Cumhuriyet University. 58140, Sivas, Turkey. Phone: +90-346-219 1010 (#3929). Fax: +90-346-219 1634. E-mail: tulayoymak@cumhuriyet.edu.tr. ORCID: https://orcid.org/0000-0001-5820-1364. Emrah Dural – ORCID: https://orcid.org/0000-0002-9320-8008

an essential step before the instrumental analysis for accurate measurement of the target analyte in a complex matrix. There are many sample preparation methods for the extraction and pre-concentration of synthetic dyes, such as solid-phase extraction (SPE), liquid-liquid microextraction (LLME), cloud point extraction (CPE), and dispersive liquid-liquid microextraction (DLLME) (Ardeshir, Foroogh, 2019; Bazregar *et al*., 2018; Heidarizadi, Tabaraki, 2016; Long *et al*., 2011; Özkan *et al*., 2019; Yoon *et al*., 2018). SPE is widely used in preparation methods because of advantages such as simplicity, low cost, good reproducibility and variety of available analytes. The choice of sorbent materials is one of the important factors in SPE procedures to achieve higher enrichment efficiency and effectively separate the target analyte from the complex matrix. There are many sorbents such as carbon nanotubes, silica gels and mesoporous silica graphene (Chen *et al*., 2013; Liu, Wang, Teng, 2005; Praveen *et al*., 2006; Qin *et al*., 2019). The dispersive solid-phase extraction procedure in which these sorbents are used requires a centrifugation step. In recent years, the use of magnetic nanoparticles (MNPs) as a sorbent has become attractive because of elimination of the centrifugation step, shortening of the duration of the extraction process, high extraction efficiency and simplicity in the application (Hu *et al*., 2019; Shariati-Rad, Haghparast, 2020; Shariati *et al*., 2011). Hence, magnetic solid-phase extraction (MSPE) has recently become important. However, MNPs also have some disadvantages such as agglomeration, poor recyclability and low selectivity. To overcome these problems, MNPs are coated with various chemical agents and natural products. The coating of MNPs provides them with important properties such as high adsorption capacity, good stability and greater surface area (Giakisikli, Anthemidis, 2013; Hidarian, Hashemian, 2014; Maddah, Shamsi, 2012; Malik *et al*., 2019; Qin, Bakheet, Zhu, 2017; Wierucka, Biziuk, 2014). Therefore, these articles have focussed on the application of coated MNPs.

In the last decade, the synthesis of MNPs with natural products has begun to be used more than chemical agents, as they are cost-effective, environmentally friendly and the resulting products are both stable and controllable (Karpagavinayagam, Vedhi, 2019; Saif, Tahir, Chen, 2016). Therefore, synthesis of MNPs using various plant extracts and discarded plant materials such as the leaves of *Camellia sinensis*, *Citrus paradisi*, peel of *Punica granatum*, orange peel, *Pisum sativum*, and flower of *Avicennia marina* have been investigated by many researchers. (Gupta, Nayak, 2012; Hoag *et al*., 2009; Karpagavinayagam, Vedhi, 2019; Kumar *et al*., 2020; Prasad, Yuvaraja, Venkateswarlu, 2017; Venkateswarlu *et al*., 2019).

Elaeagnus angustifolia is a species of the Elaeagnaceae family, which is widely used in Anatolia. The medical use of other species of the Elaeagnaceae family has been reported with applications as an analgesic, antipyretic and diuretic in traditional medicine. They have been shown to contain various compounds such as flavonoids, alkaloids, sugars and complex steroids. *E. angustifolia* fruits are not preferred as a nutrient by humans as they are physically small and wild, and have an unattractive taste. There are studies in the literature that have demonstrated that both *E. angustifolia* fruits and stones are effective adsorbent in the extraction of dyes and metals from various samples and waste-water (Kahraman, Pehlivan, 2017; Kılıç, Poyraz, 2012; Oymak, Eruygur, 2019; Tehranizadeh, Baratian, Hosseinzadeh, 2016; Yalcin, Sogut, 2014).

To date there have been no reports on the synthesis of MNPs with *E. angustifolia* fruits. In this study, for the first time, *E. angustifolia* fruits were used as capping for the synthesis of Fe_3O_4 MNPs. Synthesized Fe_3O_4-*Elaeagnus angustifolia* (EA) was used in the solid-phase extraction method for pre-concentration and separation of three synthetic dyes, and these dyes were then analyzed with high-performance liquid chromatography (HPLC) – UV detection. These synthetic dye compounds which are sunset yellow (SY), allura red (AR) and fast green (FG) were determined as target analytes to evaluate the extraction performance of this method. The characterization of the obtained materials was carried out with X-ray diffraction (XRD) and scanning electron microscopy (SEM). Various factors which affected the extraction efficiency of the method were optimized, including the influence of adsorption time, elution time, elution solvent type and volume. Finally, the suggested method was successfully used for extraction and pre-concentration of synthetic dyes in real samples.

EXPERIMENTAL

Chemicals and reagents

The analytical standard of SY (E110), AR (E129) and FG (E143) (Massachusetts, USA), 26% NH_3 solution (Steinheim, Germany), $FeSO_4.7H_2O$ (Steinheim, Germany), gradient grade acetonitrile (Missouri, USA) and 37% HCl (Austria) were purchased from Sigma-Aldrich. Ammonium acetate was purchased from Carlo Erba (Milano, Italy). $FeCl_3{\cdot}6H_2O$ and gradient grade methanol were obtained from Merck (Darmstadt, Germany). Ultrapure water was obtained from the Elga Purelab Water Purification System (Buckinghamshire, United Kingdom).

Instrumentation

Chromatographic analyses were performed by employing a Hewlett-Packard Agilent 1100 series (California, USA) high-performance liquid chromatograph (HPLC) coupled with a degasser (G1322A, Degasser), a gradient pump (G1311A, QuadPump), a column thermostat (G1316A, Colcom), a manual injector (Rheodyne 7725i) with a 20 µL loop and an ultraviolet detector (G1314A, VWD). Analytical separation was accomplished with a Zorbax C_{18} reverse-phase column (250 mm x 4.6 mm i.d., 5 µm particle size) (Delaware, USA). System control and data integration were performed with Chemstation A.08.03 software (Palo Alto, USA). pH monitorization was applied using a SevenMulti, Mettler Toledo pH-meter (Ohio, USA) combined with a glass electrode. The ultrasonic dissolving was accomplished with a Kudos OHP-SK521 model ultrasonic bath (Shanghai, China). Centrifugation was carried out with a Hettich Universal 320 model (Vestfalya, Germany) centrifuge. The characterization of the synthesized nanoadsorbent, abbreviated as Fe_3O_4-EA, was carried out with a Scanning Electron Microscope - Energy Dispersive Spectroscopy (TESCAN Mira 3XMU) a Brunauer Emmet Teller (BET) surface analyser (Quantachrome - Autosorb-1C, Florida, USA), an X-ray Diffraction (XRD) analyser (Panalytical-Empyrean, Almelo, Holland) and a Vibrating Sample Magnetometer (Lake Shore 7407, Ohio, USA).

Chromatographic conditions

Mobile phase A containing 20 mM (pH 6.7) ammonium acetate was filtered through a 0.45 µL polytetrafluoroethylene filter and then degassed by ultrasonic bath for 30 minutes. Mobile phase B was prepared with acetonitrile and methanol (1: 1, v / v). These prepared solutions were applied to the HPLC system with the gradient program described below, which has a 1 mL/min total flow rate.

In the gradient mobile phase flow program, the initial ratio of mobile phase-A and mobile phase-B were 97:3 (v/v). Subsequently, the amount of mobile phase-B component in the mobile phase was increased linearly from 3% to 97% in 16 min. The column was then conditioned for 4 min with the initial mobile phase ratios. SY and AR were detected at 500 nm and FG was detected at 600 nm with the ultraviolet detector. The unknown concentrations of SY, AR and FG were quantified using linear regression of response (analyte peak area) versus their concentrations.

Synthesis of Fe_3O_4 modified with *E. angustifolia* fruits

In this study, fruits were collected from the bottom of a wild *E. angustifolia* tree located in the Faculty of Science of Sivas Cumhuriyet University and then dried in an oven at 50ºC for 24 h. After being separated from the shells and stones by hand, they were washed several times with deionized water to remove impurities, then dried again in an oven and ground in a mortar to obtain a powder.

The dried and ground fruits of *E. angustifolia* were used in the synthesis of magnetic nanoparticles. Fe_3O_4 and Fe_3O_4-EA were synthesized using the coprecipitation method modified from that of Gupta and Nayak (2012). Briefly, 6.1 g of $FeCl_3{\cdot}6H_2O$ and 4.2 g of $FeSO_4{\cdot}7H_2O$ were dissolved in 100 mL ultrapure water and heated to 90°C. 15 mL ammonium hydroxide (26%) solution and 1.0 g of *E. angustifolia* dispersed in 100 mL ultrapure water were added rapidly and sequentially to this mixture. It was stirred at 80 °C for 30 min and then cooled to room temperature. In the final step, the black Fe_3O_4-EA precipitate obtained was collected with a powerful magnet and washed with ultrapure water several times, then dried at 60 °C for 2 h. Finally, it was stored in a polypropylene flask for further use.

MSPE procedure

Initially, 100 mg magnetic nanoadsorbent was added to a 50 mL polypropylene test tube containing 1 µg/mL of dye dissolved in 25 mL of 10 mmol/L HCl, then this mixture was stirred with the vertical tube rotator at 50 rpm for 5 min. The magnetic nanoadsorbent (containing dyes on the surface) was then separated from the suspension using a powerful magnet, and the liquid phase was removed by decanting. Then, 5 mL of methanol:1 mol/L NH_3 solution (6:4, v/v) as eluent was added to the test tube and it was vortexed at 1000 rpm for 3 min. The magnetic nanoadsorbent was held to one side of the tube by employing the powerful magnet, and the eluent solution (5 mL) was transferred to a 15 mL clean test tube. Finally, 20 µL of eluent liquid was applied to the HPLC. Each analysis was repeated individually three times and the average value was calculated.

Sample preparation

A pediatric cough syrup sample was purchased from the local pharmacy (in Sivas-Turkey). Mineral water (packaged in bottles) and colored sugar-coated chickpeas obtained from retailers were used as real samples. The pediatric syrup sample was diluted 20 times with ultrapure water. After sonication for 30 min in an ultrasonic bath, it was centrifuged at 5000 rpm for 10 min. An aliquot of 1 mL of sample was placed in the centrifuge tube and the described MSPE method was applied. The colored sugar-coated chickpeas were dispersed in 50 mL ultrapure water. After sonication for 30 min in the ultrasonic bath, the sample was centrifuged at 5000 rpm for 10 min. An aliquot of 0.5 mL of sample was placed in the test tube and the described MSPE method was applied. The mineral water sample was heated for 20 min to remove HCO_3^- prior to analysis. The described MSPE method was applied to 5 mL of the sample.

RESULTS AND DISCUSSION

Characterization of Fe_3O_4-EA

The SEM images of the *E. angustifolia*, Fe_3O_4 and Fe_3O_4-EA are shown in Figure 1. According to the EDS analysis, Fe_3O_4-EA contained 10.9% of C, 2.5% of N, 47.3% of O and 39.2% of Fe. Elemental analysis demonstrated the presence of C and N in the structure of the modified magnetic biosorbent.

The calculated BET surface area of Fe3O4 and Fe3O4 EA were 85.3 and 77.5 m2g-1, respectively. The results of the BET analysis clearly showed that Fe_3O_4 was successfully modified with *E. angustifolia*. The surface area and pore characteristics of *E. angustifolia*, Fe_3O_4 and Fe_3O_{4-}EA are given in Table I.

In the magnetometry device to measure magnetic saturation, the hysteresis curves were obtained by applying 20 kOe magnetic field at 288 K. The magnetic saturation of Fe_3O_4 and Fe_3O_4-EA magnetic particles synthesized according to the data obtained from the vibrating magnetometry device was 53.84 emu/g and 15.61 emu/g respectively. The Fe_3O_4-EA showed that when the magnetic field was applied to the magnetic particles, it can be separated easily and quickly from the aqueous medium. The measurement results for Fe_3O_4 and Fe_3O_4-EA are shown in Figure 2a. The magnetization curves of Fe_3O_4 –EA and Fe_3O_4 show that these nanoparticles are superparamagnetic.

The crystal structures of the *E. angustifolia*, Fe_3O_4 and Fe_3O_4-EA were characterized by XRD. As seen in Figure 2b, Fe_3O_4 exhibited peaks at 18.3 (111), 30.1 (220), 35.7 (311), 43.3 (400), 54.1 (422), 57.5 (511) and 62.8 (440) (Acıslı, 2019; Zhao *et al.*, 2020). The absence of the Fe_2O_3 peaks ranging from a 2θ angle of 20° to 30° was also proof that the black powder was Fe_3O_4 and therefore no impurities of Fe_2O_3 were observed in Fe_3O_4-EA (Figure 2b). The 2θ values for the Fe_3O_4 peaks of the nanocomposites were less than those of the pure Fe_3O_4, which may have been caused by the interaction between Fe_3O_4 and *E. angustifolia*.

According to the Debye–Scherrer formula, it is possible to calculate the average diameter of the nanoparticles using the XRD peak. Once the most intense peak was determined at 311, it was used to calculate the average nanoparticle diameter.

$$D_{HKL} = \frac{K * \lambda}{\beta(2\theta) * \cos(\theta)} \qquad (01)$$

Here, D_{HKL} is the mean crystallite size, K is a shape function, for which a value of 0.9 is used, λ is the wavelength of the radiation (0.154056 nm), β is the full-width at half-maximum (FWHM) value of XRD diffraction lines, θ is the half diffraction angle of 2θ (Peternele *et al.*, 2014). The average nanoparticle diameter size was calculated to be 8.8 and 12.1 nm for Fe_3O_4-EA and Fe_3O_4 respectively.

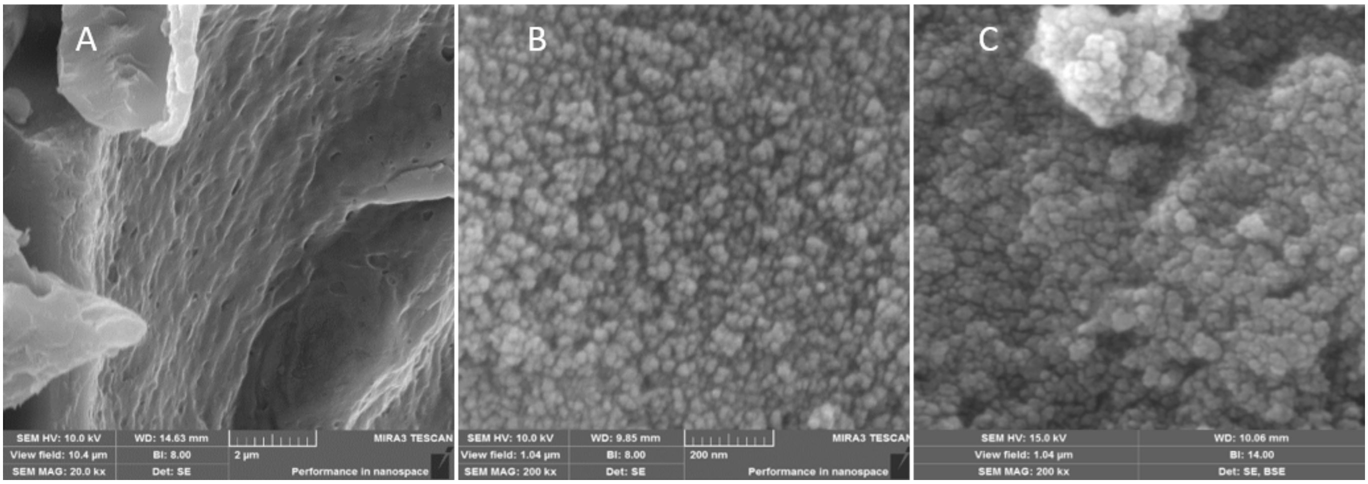

FIGURE 1 - Scanning electron microscopy for images a. *E. angustifolia*, b. Fe_3O_4, c. Fe_3O_4-EA.

TABLE I - Surface area and pore characteristics of *E. angustifolia*, Fe_3O_4 and Fe_3O_4-EA

	Surface properties		
Magnetic biosorbent	**BET surface area m²/g**	**Average pores volume cm³/g**	**Average pore diameter Å**
E. angustifolia	10.1	0.033	65.7
Fe_3O_4	85.3	0.286	57.8
Fe_3O_4-EA	77.5	0.230	51.7

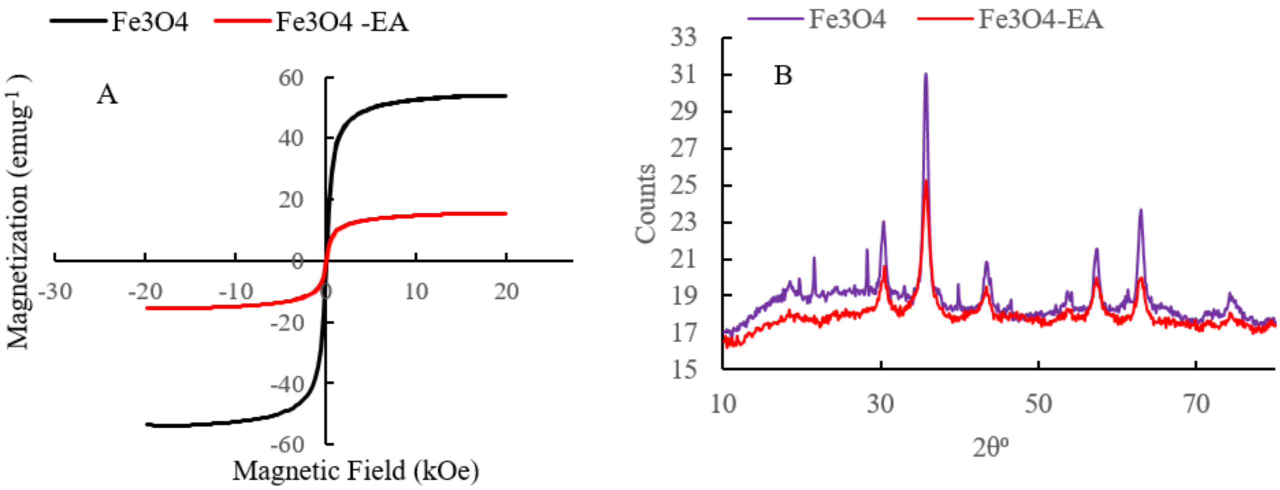

FIGURE 2a - Magnetic field curve against magnetic field strength **b.** XRD patterns of Fe_3O_4 and Fe_3O_4-EA.

Point of zero charge

Determination of the point of zero charges (pzc) of an adsorbent is very important for adsorption studies. When pH values of the solution are lower than pzc, the surface of the adsorbent is positively charged. In this case, the surface may adsorb anions. On the other hand, if the pH of the solution is higher than pzc, the surface is negatively charged and the surface may adsorb cations.

To adjust the pH of 0.1 mol/L $NaNO_3$ solution, either 0.1 mol/L HNO_3 or NaOH solution were employed (Çiftçi, 2017). To determine the pH_{pzc} of the adsorbents, the 100 mg adsorbents were added to solutions with pH levels from 2 to 11. The mixtures were shaken for 24 h. The final pH of mixtures was measured with a pH meter and ΔpH values were calculated.

The graph of ΔpH versus the initial pH is given in Figure S1. As shown in Figure S1, the zero point charge of pH values was determined as 4.0 for Fe_3O_4-EA. When pH <4.0, the surface of Fe_3O_4-EA becomes positively charged and is feasible for adsorption of anionic species such as SY, AR and FG.

Optimization of MSPE conditions

Solution acidity affects the adsorption and desorption of the analytes on the sorbent. The effect of pH on the MSPE of dyes was investigated using hydrochloric acid. The HCl concentrations were studied by varying the 2-50 mmol/L for the quantitative determination of SY, AR, and FG. The 10 mmol/L was selected as the optimum for further investigation. Recovery values were found to be 102%,101%, and 86%, respectively for SY, AR, and FG. The results are given in Figure 3a.

For the quantitative recovery of the adsorbed analytes, a suitable eluent must be used. For this purpose, 100 mg magnetic biosorbent and 1 µg/mL of dyes containing 25 mL of 10 mM HCl model solution were applied to the procedure using a different desorption solution. The results are given in Figure 3b. For the quantitative extraction of all the dyes, 5 mL of 40% 1 M NH_3 60% methanol was selected as the eluent. The effect of eluent types on recovery SY, AR and FG are given in Figure 3b.

The effect of the adsorption time on the adsorption of synthetic dyes by Fe_3O_4-EA was studied (25 mL, 1 µg/mL dye solution) with 100 mg of the sorbent over a series of varying shaking times (0–15 min). The results showed that the percentage extraction of synthetic dyes at 5 min and higher than 98%. The effect of the elution time on the adsorption of synthetic dyes by Fe_3O_4-EA (25 mL, 1 µg/mL) was examined with 100 mg of the sorbent and adsorption of 5 min over a series of varying shaking times (0–10 min). Accordingly, in all subsequent experiments for quantitative sorption and elution of synthetic dyes, 3 min and 5 min were used.

Adsorption and desorption cycle experiments were investigated for the reusability of Fe_3O_4-EA for MSPE of dyes. The results indicated that the recovery of dyes was quantitative for 60 cycles. The mean recovery % values with standard deviation for 60 runs were found to be 97.6 ± 4.3, 97.3 ± 4.6, 96.0 ± 4.8 for SY, AR, and FG, respectively. These results show that the magnetic nanoadsorbent was mechanically stable and has an excellent reusability.

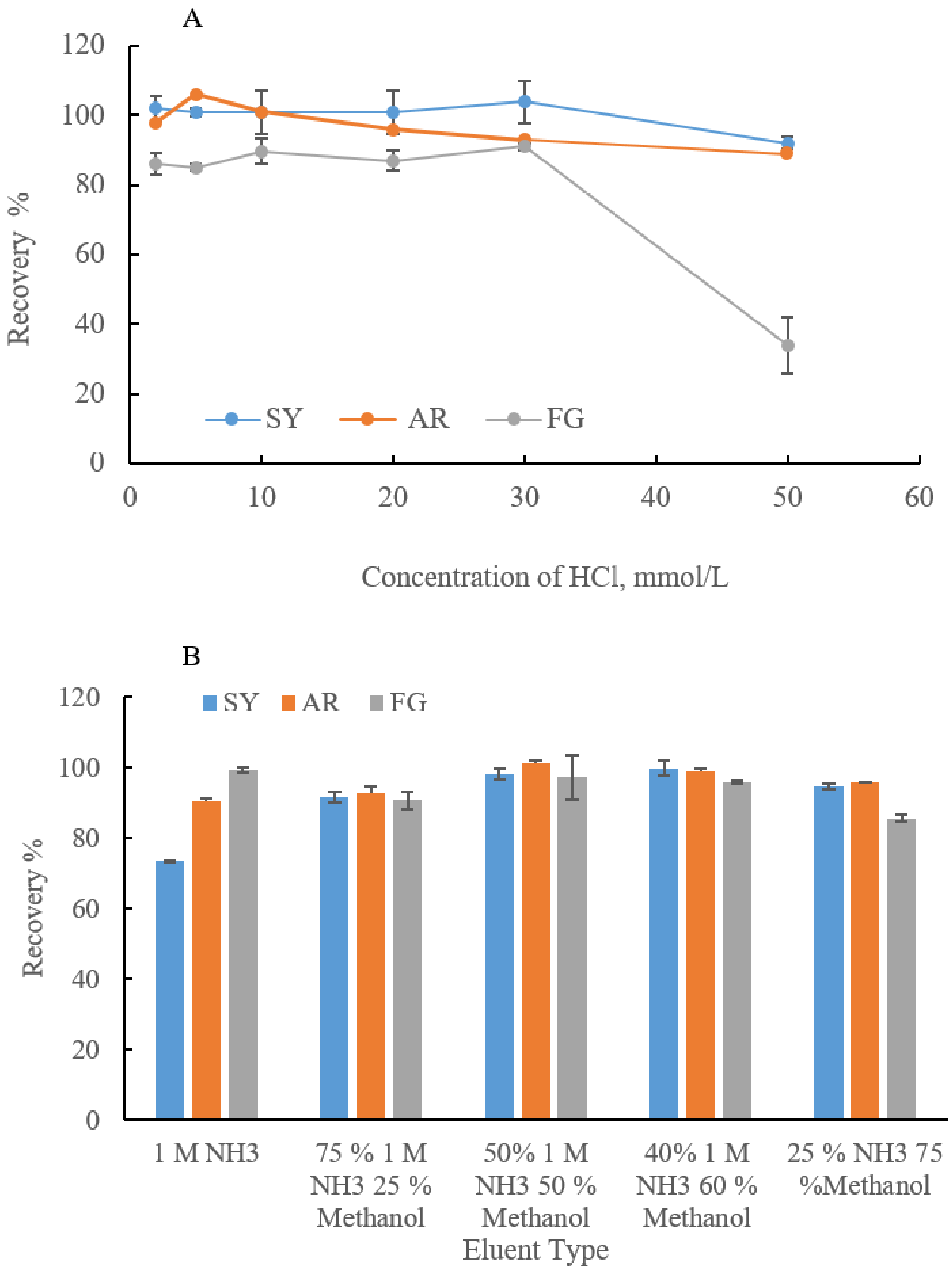

FIGURE 3A - Effect of HCl concentration on extraction of dyes (100 mg Fe_3O_4-EA, 1 µg/mL of dyes containing 25 mL solution, eluent: 25% NH_3 75% Methanol) **3B** - Effect of eluent types on recovery SY, AR and FG on Fe_3O_4-EA (100 mg Fe_3O_4-EA, 1 µg/ mL of dyes containing 25 mL 10 mmol/ L HCl solution).

Adsorption capacity of Fe_3O_4-EA and comparison with Fe_3O_4

In order to examine the adsorption behaviour of the Fe_3O_4 and Fe_3O_4-EA, the SY, AR and FG were added to the model solution at increasing concentrations (100 µg/mL to 600 µg/mL). The adsorption capacity study of SY, AR, and FG by the Fe_3O_4 and -Fe_3O_4-EA was determined for each dye individually with a batch approach. The aqueous solutions of 25 mL dyes were shaken for 12 h in a shaker. The sorbents and aqueous solutions were separated by the magnet and the supernatant solution was diluted. The dye concentration in the solution was determined with a UV–Vis spectrophotometer at 480 nm, 510 nm, 624 nm for SY, AR and FG, respectively.

Figure 4. shows the adsorption isotherm which conforms to the Langmuir equation. The adsorption capacity (q_m) and the binding equilibrium constant (K) of sorbents for each dye was calculated from the Langmuir equation. This equation 1 can be given in the following form:

$$\frac{C_e}{q_e} = \frac{1}{q_m K} + \frac{1}{q_m} C_e \qquad (02)$$

The Langmuir adsorption parameters are given in Table II. Since the Langmuir isotherm assumes that adsorption takes place in a single layer, the separation factor R_L indicates the type of the isotherm. R_L is calculated as given in the following equation.

$$R_L = \frac{1}{1 + K_L * C_0} \qquad (03)$$

It is an indication that if the R_L value is greater than 1.0, the isotherm is unsuitable. The fact that the R_L values are in the range of 0-1 indicates that adsorption is suitable. (Baytar, Ceyhan 2018; Yagub *et al.*, 2014). Both Fe_3O_4-EA and Fe_3O_4 are suitable for the adsorption of the SY, AR and FG. Table S1 shows the effect of initial dye concentration on the R_L value. The adsorption capacity values of Fe_3O_4-EA are higher compared to Fe_3O_4 for dyes. The smaller size adsorbents have better dispersion and suspension in the aqueous solution. Thus, the interaction between analyte and sorbent increases. The average nanoparticle diameter of Fe_3O_4-EA is 8.8 nm and smaller than the average nanoparticle diameter of Fe_3O_4,which is 12.1 nm. The average pore size and pore diameter of Fe_3O_4-EA is smaller than that of Fe_3O_4. The fact that Fe_3O_4-EA has a small nanoparticle diameter and decreased pore size and pore diameter caused an increase in the amount of adsorbed dyes. The adsorption capacity values are given in Table II.

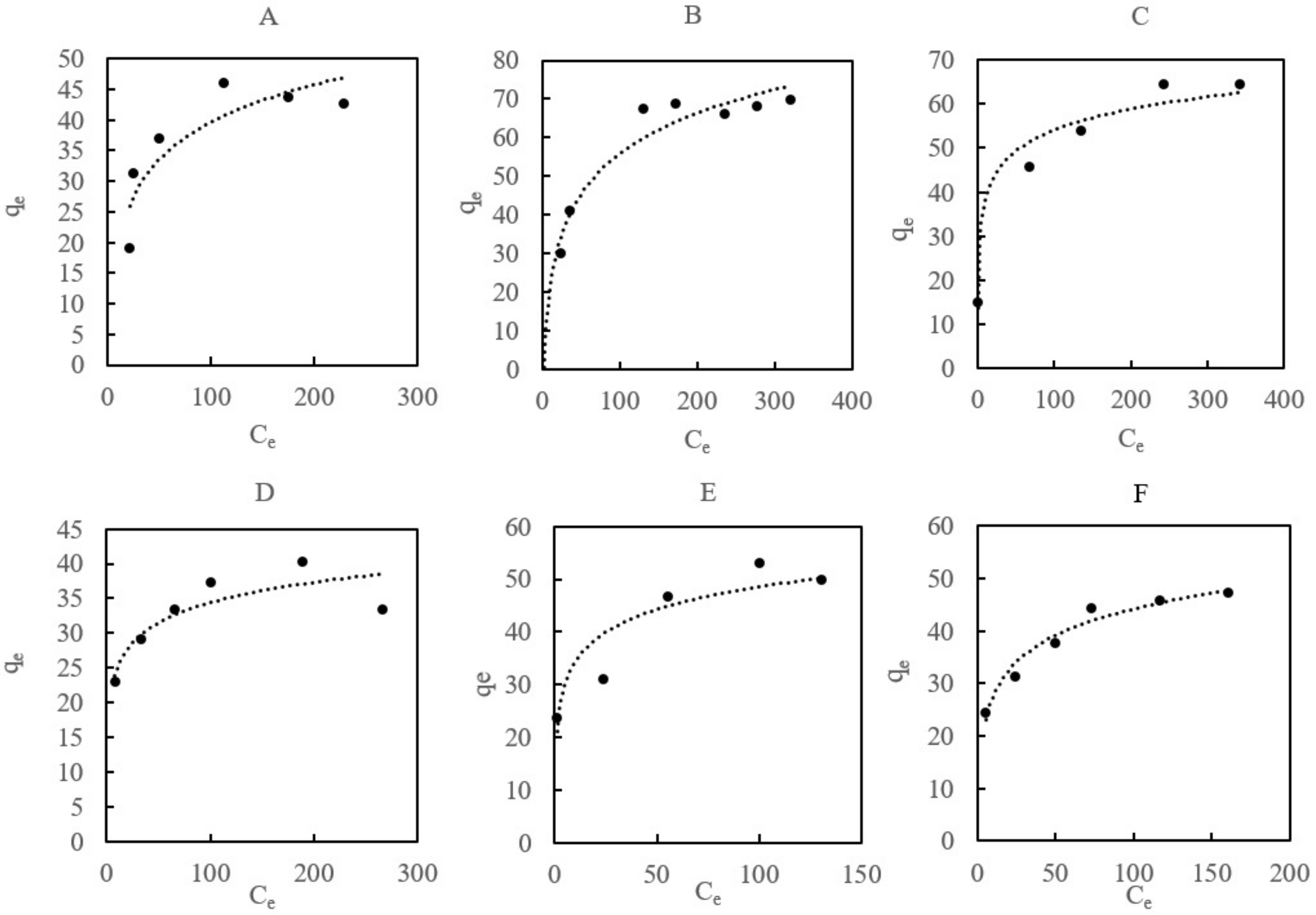

FIGURE 4 - Adsorption capacity of Fe_3O_4-EA for SY (a), AR (b), FG (c) and Fe_3O_4 for SY (d), AR (e), FG (f).

TABLE II - Adsorption constants for SY, AR and FG on Fe_3O_4-EA and Fe_3O_4

Adsorbent	Dyes	Langmuir Parameters		
		q_m (mg/g)	K_L (L/mg)	r^2
Fe_3O_4-EA	SY	45.0	0.13	0.9946
	AR	70.4	0.14	0.9953
	FG	73.0	0.05	0.9949
Fe_3O_4	SY	33.7	1.17	0.9978
	AR	52.4	0.28	0.9929
	FG	52.6	0.06	0.9984

METHOD VALIDATION

This analytical method was validated according to ICH Harmonised Tripartite Guideline Q2 (R1), the "Validation of Analytical Procedures: Text and Methodology" in terms of linearity, accuracy, precision, sensitivity and recovery (2005). The mathematical ratio of analyte concentrations to peak areas was used in all validation calculations.

The method was validated using spiked ultrapure water samples. Under optimized parameters, good linearity was achieved between 1 to 20 μg/mL against three dye samples at 5 different concentration levels and coefficients of determination (r^2) were between 0.9981 and 0.9999 by linear regression. Chromatograms of the dye standards are given in Figure S2, which shows the high resolution with no interference in a relatively short separation time (13 min) for 3 dyes. System suitability parameters are given in Table III. The accuracy, defined as the relative error (RE) was calculated as the percentage difference between the added and found of analyte/dye quantity by five separate replicates both intraday and inter-day.

The limit of detection (LOD) and limit of quantification (LOQ) were calculated according to the ICH recommendations (2005) based on standard deviation of the response and the slope of the calibration graph (LOD = 3.3; LOQ = 10). In the sensitivity test, 0.2 μg / mL as the lowest calibration point of the analytes was used. LOD and LOQ values of SY, AR and FG were calculated as 0.07, 0.05, 0.1 and 0.21, 0.15, 0.31, respectively, and the pre-concentration factor value was considered as "5" in all analyses. Intraday and inter-day repeatability were detected between (-10.9) – 7.7 and (-8.8) – 7.1 (RE), respectively (Table S2). The precision, defined as relative standard deviation (RSD), was calculated from five separate replicates of SY, AR and FG both intraday and inter-day. Five replicate spiked samples individually prepared were assayed at the three different concentrations (0.2, 1.0 and 2.0 μg/mL) for all analytes. As shown in Table S2, intraday and inter-day repeatability was detected as 6.9 and 8.1 (RSD). The chromatographic characteristics and system suitability parameters are summarized in Table III.

TABLE III - Chromatographic characteristics and system suitability parameters

	SY	**AR**	**FG**
Linear range (μg/mL)	1 – 20	1 – 20	1 – 20
Calibration equation	y = 58.579x + 47.894	y = 109.8x + 2.9872	y = 145.04x + 23.464
Coefficient of determination (r^2)	0.9981	0.9995	0.9999
Retention time (t_R)	9.6	10.5	12.5
Capacity factor (k')	1.3	1.6	2.0
Theoretical plate number (*N*)	2256	2756	3086
Resolution (R_s)	6.8	1.3	2.4
Specificity factor (α)	2.3	2.6	3.0
LOD (μg/mL)	0.07	0.05	0.10
LOQ (μg/mL)	0.21	0.15	0.31

Capacity factor (k') = $\frac{tR-t0}{t0}$; Theoretical plate number (*N*) = $16(\frac{tR}{Wt})^2$; Resolution (R_s) = $\frac{\sqrt{N}}{4}\,\frac{(\alpha-1)}{\alpha}\,\frac{k}{(k+1)}$; Specificity factor (α) = $\frac{k2}{k1}$. Abbreviations: t_R: retention time of the analyte peak; t_0: retention time of mobile phase peak; WT: peak width

Accuracy of the method and analysis of real samples

To investigate the reliability and accuracy of the described method, the analyses of the real samples together with recovery experiments were carried out. For this purpose, dyes of known concentrations were added to the real samples and analyzed after applying the described method. The results are summarized in Table IV and chromatograms of dye real samples are given in Figure S3. As seen in Table IV, the recovery values of the dyes in the samples were found to range from 82.5% to 103.5%. The mean dye concentrations ± standard deviation in the samples (n = 3) were found to be 1.81 ± 0.10 mg/g for colored sugar-coated chickpeas and 0.73± 0.01 µg/mL for child syrup. No dye concentration was detected in the mineral water.

TABLE IV - Determination of SY, AR and FG in samples, pH 2; eluent, 5 mL of methanol/1 M NH_3 (6/4, v/v); 100 mg Fe_3O_4-EA

Sample Name		SY		AR		FG	
	Added (µg/mL)	Founded $\bar{x}$ ± SD (µg/mL)	R (%)	Founded $\bar{x}$ ± SD (µg/mL)	R (%)	Founded $\bar{x}$ ± SD (µg/mL)	R (%)
Colored Sugar-coated Chickpeas	0	3.38±0.19	-	ND	-	ND	-
	2	5.45±0.38	103.5	1.96±0.22	98.2	1.72±0.32	86.0
	5	8.35±0.98	99.5	5.01±0.03	100.2	4.94±0.15	98.8
Pediatric Syrup	0	0.73±0.01	-	ND	-	ND	-
	2	2.66±0.19	96.3	1.96±0.13	98.0	1.65±0.011	82.5
	4	4.51±0.04	94.5	3.87±0.25	96.7	3.72±0.28	93.0
Mineral Water	0	ND	-	ND	-	ND	-
	2	1.80±0.04	90.1	1.84±0.50	92.2	1.74±0.07	87.2
	5	5.02±0.04	100.4	4.89±0.20	97.8	4.96±0.18	99.2

Results are the average of three experiments (n=3), SD: Standard deviation, R: Recovery, ND: Not detected

CONCLUSION

In this study, a new magnetic adsorbent Fe_3O_4-EA was synthesized and using the Fe_3O_4-EA, the MSPE method was developed and optimized for the determination of three anionic dyes with HPLC. Sample chromatograms of the dyes before and after the MSPE method are given in Figure S4. This method was simple and rapid. The MSPE procedure took approximately 10 minutes. The short extraction procedure, simple operation, and good reusability (≤60 times) were advantages of the proposed method. The MSPE was successfully employed in the analysis of real samples of paediatric syrup, colored sugar-coated chickpeas, and mineral water. The magnetic nanoadsorbent exhibited promising performance in MSPE of anionic dyes, and the strategy of using Fe_3O_4-EA as a sorbent in extraction is ongoing.

ACKNOWLEDGMENTS

This work was conducted in the Sivas Cumhuriyet University, Faculty of Medicine Research Center (CÜTFAM) and therefore, the authors would like to thank all personnel in CÜTFAM for their open collaboration.

REFERENCES

Acıslı O. Comparison of the removal efficiencies of Acid Blue 185 dye through adsorption, Fenton and photo-Fenton-like processes over the natural hematite, siderite and magnetite minerals containing different amounts of iron. Eur J Sci Technol. 2019;(15):199-209.

Ali MY, Hassan GM, Hassan AMS, Mohamed ZA, Ramadan MF. In vivo genotoxicity assessment of sunset yellow and sodium benzoate in female rats. Drug Chem Toxicol. 2020;43(5):504-513.

Allam KV, Kumar GP. Colorants - the cosmetics for the pharmaceutical dosage forms. Int J Pharm Pharm Sci. 2011;3(3):13-21.

Amchova P, Kotolova H, Ruda-Kucerova J. Health safety issues of synthetic food colorants. Regul Toxicol Pharmacol. 2015;73(3):914-922.

De Andrade FI, Florindo Guedes MI, Pinto Vieira ÍG, Pereira Mendes FN, Salmito Rodrigues PA, Costa Maia CS, et al. Determination of synthetic food dyes in commercial soft drinks by TLC and ion-pair HPLC. Food Chem. 2014;157:193-198.

Ardeshir Shokrollahi, Foroogh Ebrahimi. Simultaneous determination of brilliant green and basic fuchsin by cloud point extraction–scanometry. J Anal Chem. 2019;74(10):1019-1026.

Baytar O, Ceyhan AA. Adsorption of methylene blue by magnetic NiFe2 O4 / activated carbon nanocomposite: kinetics and isotherm. Selcuk Univ J Eng Sci Technol. 2018;6(2):227-241.

Bazregar M, Rajabi M, Yamini Y, Arghavani-Beydokhti S, Asghari A. Centrifugeless dispersive liquid-liquid microextraction based on salting-out phenomenon followed by high performance liquid chromatography for determination of Sudan dyes in different species. Food Chem. 2018;244:1-6.

Chen R, Zhao T, Lu J, Wu F, Li L, Chen J, et al. Graphene-based three-dimensional hierarchical sandwich-type architecture for high-performance Li/S batteries. Nano Lett. 2013;13(10):4642-9.

Çiftçi TD. Adsorption of Cu(II) on three adsorbents, Fe_3O4/Ni/Nix nanocomposite, carob (Ceratonia siliqua), and grape seeds: A comparative study. Turkish J Chem. 2017;41(5):760-772.

EFSA Panel on Dietetic Products, Nutrition and Allergies (NDA). Scientific Ooinion on the appropriateness of the food azo-colours Tartrazine (E 102), Sunset Yellow FCF (E 110), Carmoisine (E 122), Amaranth (E 123), Ponceau 4R (E 124), Allura Red AC (E 129), Brilliant Black BN (E 151), Brown FK (E 154), Brown HT (E 155). EFSA J. 2010;8(10):1778.

Giakisikli G, Anthemidis AN. Magnetic materials as sorbents for metal/metalloid preconcentration and/or separation. A review. Anal Chim Acta. 2013;789:1-16.

Gupta VK, Nayak A. Cadmium removal and recovery from aqueous solutions by novel adsorbents prepared from orange peel and Fe2O3 nanoparticles. Chem Eng J. 2012;180:81-90.

He G, Evers S, Liang X, Cuisinier M, Garsuch A, Nazar LF. Tailoring porosity in carbon nanospheres for lithium-sulfur battery cathodes. ACS Nano. 2013;7(12):10920-10930.

Heidarizadi E, Tabaraki R. Simultaneous spectrophotometric determination of synthetic dyes in food samples after cloud point extraction using multiple response optimizations. Talanta. 2016;148:237-246.

Hidarian M, Hashemian S. Synthesize and characterization of sawdust/MnFe2O4Nano composite for removal of indigo carmine from aqueous solutions. Orient J Chem. 2014;30(4):1753-1762.

Hoag GE, Collins JB, Holcomb JL, Hoag JR, Nadagouda MN, Varma RS. Degradation of bromothymol blue by 'greener' nano-scale zero-valent iron synthesized using tea polyphenols. J Mater Chem. 2009;19(45):8671-8677.

Hu K, Qiao J, Zhu W, Chen X, Dong C. Magnetic naphthalene-based polyimide polymer for extraction of Sudan dyes in chili sauce. Microchem J. 2019;149(156):104073.

Hu M, Huang P, Huang W, Wu F. Fe_3O4 Magnetic Nanoparticles modified with sodium dodecyl sulfate for removal of basic orange 21 and basic orange 22 from complex food samples with high-performance liquid chromatographic analysis. Food Anal Methods. 2017;10(9):3119-3127.

Iammarino M, Mentana A, Centonze D, Palermo C, Mangiacotti M, Chiaravalle AE. Simultaneous determination of twelve dyes in meat products: Development and validation of an analytical method based on HPLC-UV-diode array detection. Food Chem. 2019;285:1-9.

International Conference on Harmonisation. Valid. Anal. Proced. Text Methodol. Q2(R1). 2005. p. 1–17.

Kahraman HT, Pehlivan E. Cr 6 + removal using oleaster (Elaeagnus) seed and cherry (Prunus avium) stone biochar. Powder Technol. 2017;306:61-67.

Karpagavinayagam P, Vedhi C. Green synthesis of iron oxide nanoparticles using *Avicennia marina* flower extract. Vacuum. 2019;160:286-292.

Kılıç M, Poyraz Z. *Elaeagnus angustifolia* stone as a low-cost biosorbent precursor for removal of methylene blue from aqueous solution. Anadolu Univ J Sci Technol-A. 2012;13(1)13-21.

Kumar B, Smita K, Galeas S, Sharma V, Guerrero VH, Debut A, et al. Characterization and application of biosynthesized iron oxide nanoparticles using *Citrus paradisi* peel: A sustainable approach. Inorg Chem Commun. 2020;119:108116.

Liu HY, Wang KP, Teng H. A simplified preparation of mesoporous carbon and the examination of the carbon accessibility for electric double layer formation. Carbon. 2005;43(3):559-566.

Long C, Mai Z, Yang X, Zhu B, Xu X, Huang X, et al. A new liquid-liquid extraction method for determination of 6 azo-dyes in chilli products by high-performance liquid chromatography. Food Chem. 2011;126(3):1324-1329.

López-de-Alba PL, López-Martínez L, De-León-Rodríguez LM. Simultaneous determination of synthetic dyes tartrazine, allura red and sunset yellow by differential pulse polarography and partial least squares. A multivariate calibration method. Electroanalysis. 2002;14(3):197-205.

Maddah B, Shamsi J. Extraction and preconcentration of trace amounts of diazinon and fenitrothion from environmental water by magnetite octadecylsilane nanoparticles. J Chromatogr. A. 2012;1256:40-45.

Malik R, Goyal A, Yadav S, Gupta N, Goel N, Kaushik A, et al. Functionalized magnetic nanomaterials for rapid and effective adsorptive removal of fluoroquinolones: Comprehensive experimental cum computational investigations. J Hazard Mater. 2019;364:621-634.

Mathiyalagan S, Mandal BK, Ling YC. Determination of synthetic and natural colorants in selected green colored foodstuffs through reverse phase-high performance liquid chromatography. Food Chem. 2019;278:381-387.

McCann D, Barrett A, Cooper A, Crumpler D, Dalen L, Grimshaw K, et al. Food additives and hyperactive behaviour in 3-year-old and 8/9-year-old children in the community: a randomised, double-blinded, placebo-controlled trial. Lancet. 2007;370(9598):1560-1567.

Oymak T, Eruygur N. Effective and rapid removal of cationic and anionic dyes from aqueous solutions using *Elaeagnus angustifolia* L.fruits as a biosorbent. Desalin Water Treat. 2019;138:257-264.

Özkan BÇ, Fırat M, Chormey DS, Bakırdere S. Accurate and sensitive determination of harmful aromatic amine products of azo dyes in wastewater and textile samples by GC–MS after multivariate optimization of binary solvent dispersive liquid-liquid microextraction. Microchem J. 2019;145:84-89.

Peternele WS, Monge Fuentes V, Fascineli ML, Rodrigues Da Silva J, Silva RC, Lucci CM, et al. Experimental investigation of the coprecipitation method: An approach to obtain magnetite and maghemite nanoparticles with improved properties. J Nanomater. 2014;(1):1-11.

Prasad C, Yuvaraja G, Venkateswarlu P. Biogenic synthesis of Fe_3O4 magnetic nanoparticles using *Pisum sativum* peels extract and its effect on magnetic and Methyl orange dye degradation studies. J Magn Magn Mater. 2017;424:376-381.

Praveen RS, Daniel S, Rao TP, Sampath S, Rao KS. Flow injection on-line solid phase extractive preconcentration of palladium(II) in dust and rock samples using exfoliated graphite packed microcolumns and determination by flame atomic absorption spectrometry. Talanta. 2006;70(2):437-443.

Qin P, Yang Y, Li W, Zhang J, Zhou Q, Lu M. Amino-functionalized mesoporous silica nanospheres (MSN-NH 2) as sorbent for extraction and concentration of synthetic dyes from foodstuffs prior to HPLC analysis. Anal Methods. 2019;11(1):105-112.

Qin X, Bakheet AAA, Zhu X. Fe_3O4@ionic liquid-β-cyclodextrin polymer magnetic solid phase extraction coupled with HPLC for the separation/analysis of congo red. J Iran Chem Soc. 2017;14(9):2017-2022.

Rovina K, Prabakaran PP, Siddiquee S, Shaarani SM. Methods for the analysis of Sunset Yellow FCF (E110) in food and beverage products- a review. Trends Anal Chem. 2016;85(Pt B):47-56.

Saif S, Tahir A, Chen Y. Green synthesis of iron nanoparticles and their environmental applications and implications. Nanomaterials. 2016;6(11):1-26.

Sayed HM, Fouad D, Ataya FS, Hassan NHA, Fahmy MA. The modifying effect of selenium and vitamins A, C, and E on the genotoxicity induced by sunset yellow in male mice. Mutat Res - Genet Toxicol Environ Mutagen. 2012;744(2):145-153.

Shariati-Rad M, Haghparast N. Synthesis of a novel magnetic nanocomposite and its application to the efficient preconcentration and determination of Malachite Green in fish samples using response surface methodology. Anal Bioanal Chem Res. 2020;7(1):131-150.

Shariati S, Faraji M, Yamini Y, Rajabi AA. Fe_3O4 magnetic nanoparticles modified with sodium dodecyl sulfate for removal of safranin O dye from aqueous solutions. Desalination. 2011;270(1–3):160-5.

Tehranizadeh ZA, Baratian A, Hosseinzadeh H. Russian olive (*Elaeagnus angustifolia*) as a herbal healer. Tabriz Univ Med Sci. 2016;6(3):155-167.

Tikhomirova TI, Ramazanova GR, Apyari V V. Effect of nature and structure of synthetic anionic food dyes on their sorption onto different sorbents: Peculiarities and prospects. Microchem J. 2018;143:305-311.

Venkateswarlu S, Kumar BN, Prathima B, SubbaRao Y, Jyothi NVV. A novel green synthesis of Fe_3O_4 magnetic nanorods using *Punica granatum* rind extract and its application for removal of Pb(II) from aqueous environment. Arab J Chem. 2019;12(4):588-596.

Vlase L, Muntean D, Cobzac SC, Lorena F. Development and validation of an HPLC-UV method for determination of synthetic food colorants. Rev Roum Chim. 2014;59(9):719-725.

Wierucka M, Biziuk M. Application of magnetic nanoparticles for magnetic solid-phase extraction in preparing biological, environmental and food samples. Trends Anal Chem. 2014;59:50-58.

Yadav A, Kumar A, Dwivedi PD, Tripathi A, Das M. *In vitro* studies on immunotoxic potential of Orange II in splenocytes. Toxicol Lett. 2012;208(3):239-245.

Yagub MT, Sen TK, Afroze S, Ang HM. Dye and its removal from aqueous solution by adsorption: A review. Adv Colloid Interface Sci. 2014;209:172-184.

Yalcin G, Sogut O. Antioxidant capacity of *Elaeagnus angustifolia* L. and investigation of eosin y as the fluorescent probe in ORAC method. J Food Agric Environ. 2014;12(2):51-54.

Yoon J, Kim Y, Kim K-B, Park EJ, Na DH. Reversed-phase high-performance liquid chromatographic method for the determination of permaton red (D&C Red No. 36) in cosmetics. Bull Korean Chem Soc. 2018;39(10):1219-1222.

Zhao Y, Wu R, Yu H, Li J, Liu L, Wang S, et al. Magnetic solid-phase extraction of sulfonamide antibiotics in water and animal-derived food samples using core-shell magnetite and molybdenum disulfide nanocomposite adsorbent. J Chromatogr A. 2020;1610.

Received for publication on 25th September 2020
Accepted for publication on 15th May 2021